

A TWO-DIMENSIONAL WIRE SCANNER FOR A LOW ENERGY ION BEAM

C. Gabor*, RAL, ASTeC, Chilton, Didcot, Oxfordshire, UK
 G. Boorman, Royal Holloway University of London, Surrey, UK
 A.P. Letchford, RAL, ISIS, Chilton, Didcot, Oxfordshire, UK

Abstract

The Front End Test Stand (FETS) at the Rutherford Appleton Laboratory (RAL) is intended to demonstrate the early stages of acceleration for future high power proton applications. So far, the H^- ion source and the Low Energy Beam Transport (LEBT) are operational. The commissioning of the LEBT is carried out with a multi-purpose diagnostics vessel. On the other hand, the present status of the LEBT does not provide any permanent installed beam diagnostics beyond current measurement. Possible diagnostics need to be compact and rigid in a way that it can survive an area with potentially beam losses producing residual gas ions and not suffering of beam noise. Furthermore, minimal invasive diagnostics is preferred. It is intended to present first results of a wire scanner where the geometry has been changed in a way that the two dimensional xy-space is accessible.

INTRODUCTION

FETS is a beamline to demonstrate a high current, fast chopped H^- ion beam at 3 MeV [1]. An overview is shown in Fig. 1. The beamline so far comprises the operational ion source with a slit extraction and a Post Acceleration System (PA), the LEBT up till the injection of the RFQ. Here, a multi-purpose diagnostics vessel is installed instead to perform emittance measurements. It is planned to carry out first tests with the RFQ by early next year. A complementary part of FETS are activities of using photo-detachment (PD) for non-destructive beam diagnostics because of the high power density and the advantage of further use of the beam during the actual measurement [2, 3].

For the beam instrumentation at the LEBT, the first pumping vessel after the ion source was tailored to install a PD

* christoph.gabor@stfc.ac.uk

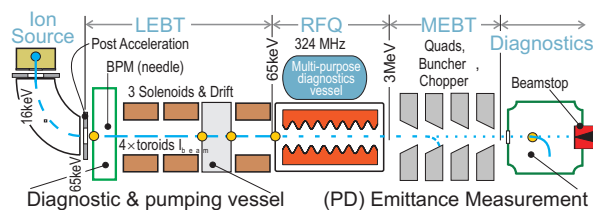


Figure 1: Overview of the FETS beamline. 4 Toroids are used for beam current and shown as dots. The needle-BPM is placed in the pumping vessel in front of the first solenoid (approx 25 mm downstream of the PA). This is the closest point to the ion source to measure the extracted beam.

Beam Profile Monitor (BPM) with in total up to 4 linear and 4 rotary vacuum suitable, piezo-driven stages to move mirrors to scan the beam with a laser. However, some problems were underestimated and are discussed in [4, 5]. So, it was considered to re-use the existing hardware to build a BPM based on a thick wire to have enough stability to support only one end: This enables free translation and rotation through the beam, should withstand the power density of the beam and despite a mechanical part in the beam it is still minimal invasive. For the remaining part of the paper this idea will be discussed in more depth and first experimental results shown where the needle was used to take profiles $I(x)$.

CONCEPTUAL DESIGN

Tomography means to reconstruct a 2D distribution based on several projections under different angles and is widely known e.g. in clinical applications where a standard method is the filtered back-projection [6]. More advanced algorithms can handle a limited number of projections $n < 5 \dots 12$ with a low number of data points (voxel: 30... 200) better; one example is a Bayesian technique called Maximum Entropy. This code is already in use and was tested in [7] for tomographic reconstruction in phase space as well as real space.

In Fig. 2 (A) the parameters r and θ are introduced. A parallel projection is shown where for constant θ the beam is probed varying r and taking profiles $I(r, \theta_{const})$ (1st generation tomography). But e.g. medical applications like CT

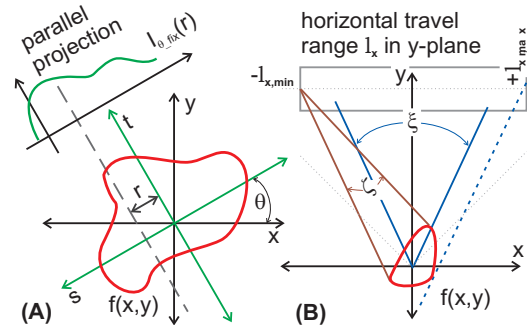


Figure 2: (A) Shows the two parameters r and θ to be varied for tomographic reconstruction (parallel projection). Full tomographic reconstruction requires 180° or if split into 2 planes each must cover 90°. (B): Full range of 90° for one plane cannot be covered by parallel projections only if the travel range is limited. But it is possible to vary θ such that r depends on $r(\theta)$ to improve the scanning range.

are more sophisticated geometries (fan geometry) in use where at the same time r and θ are varied with the advantage of more voxel per time with profiles $I(r, \theta)$. Beside the number of voxel it is also decisive that the full angle of $\theta = 180^\circ$ is evenly covered. Alternatively, this can be split in two units each installed in a transversal plane. Then ideal coverage would mean $\theta x, y = 90^\circ$ for each plane.

A similar idea is shown in Fig. 2(B) in order to extend the

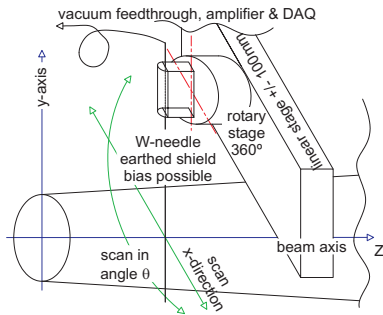


Figure 3: Sketch of the arrangement of linear and rotary stage. Set-up shown for only one plane, here the horizontal x-plane.

limitations coverage usually arising due to technical and practical constraints in beam instrumentation. To move a wire through the beam both a linear and rotary stage are necessary. Due to a finite travel range (here ± 100 mm) the wire cannot be moved any more through the beam if a certain angle is exceeded. If a beam of $\varnothing 50$ mm is assumed than the maximum coverage in angle is $\approx \pm 50^\circ$ for the given set-up. But improvements are possible if the x-position is kept constant and the rotary stage carries out a sweep, $I_r(\theta)(\theta)$. This would add another $\approx 32^\circ$. Note, that both θ and r are varied but r is not independent any more. The complete arrangement of the two stages for one plane is shown in Fig. 3. A second plane should be installed for good reconstruction.

EXPERIMENTAL SET-UP

A picture of the arm which is moved is shown in Fig. 4. The wire or better needle is $\varnothing 1.6$ mm thick and 120 mm are exposed to the beam. About 50 mm is needed for the mounting, contact and insulation. Solely for simplicity, welding electrodes of a W-alloy (EWTH-2) were used and

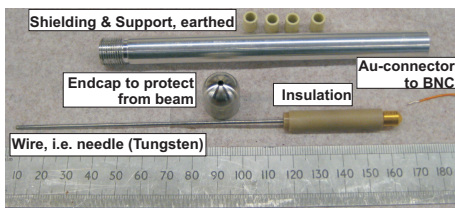


Figure 4: Picture of the Tungsten rod (1.6 mm), insulation, shielding and electrical contact leading to a 50Ω vacuum feed through.

will be replaced by pure Tungsten.

The stage, manufactured by Heason, has a range of 200 mm and with a Renshaw encoder attached. The stage and encoder are controlled by a DeltaTau PMAC2 controller with a USB interface connected to the DAQ PC.

The needle is capacitively coupled to some electronics consisting of a op-amp buffer. It is possible to add a bias of up to 500 V to the needle should it be necessary. The circuit was simulated using current generator IG1 representing a current from the needle in the H-minus beam, set to $100 \mu\text{A}$ pulse height and width $200 \mu\text{s}$. The output is a pulse of about -15 mV , with an offset of a few mV. The rise and fall times are about $25 \mu\text{s}$. The output from the electronics goes to a differential ADC channel on a USB-DAQ unit (National Instruments USB-6008 was used for initial tests).

The bandwidth (BW) of the signal is approximately $0.35/\text{risetime}$, equating to 14 kHz . To adequately sample the signal, the sample rate needs to be at least twice the signal's bandwidth, equating to a minimum of 28 kSa/s . The USB-6008 has a maximum sample rate of 10 kSa/s , and so pulse definition will be lost when sampled using this DAQ device. The minimum input voltage range for the USB-6008 is 2 V , with a 12-bit input resolution This equates to a minimum detectable voltage change of $2\text{V}/2^{12} = 0.49 \text{ mV}$. The system noise for the 2 V range is $0.5 V_{\text{rms}}$, and a full-scale absolute accuracy of 1.53 mV . The total noise is therefore $\sqrt{(0.49^2 + 0.5^2 + 1.53^2)} = 1.7 \text{ mV}$. For a 15 mV signal this equates to an error of just over 11% during AD conversion.

Stage movement and data acquisition is controlled by a program written in LabVIEW. The needle is stepped through the H^- beam and ADC data recorded at the each needle position. The ADC takes a requested number of samples, at a rate of 10 kSa/s , at each position, and writes the ADC data and stage position to file for later analysis.

FIRST EXPERIMENTAL EXPERIENCES

Examples of 1D beam profile $I(x)$ are shown in Fig. 5. The measured signal was under all circumstances negative, even if a bias was applied. Therefore at least very high secondary electron emission can be out ruled. Notable are the high intensity with a prominent peak and a relatively low intensity but large tail. This is consisted with other

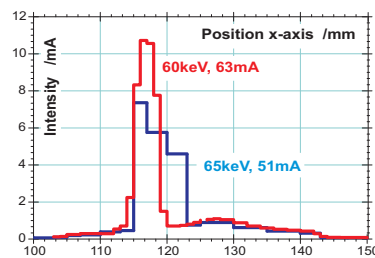


Figure 5: Example of two beam pulses $I(x)$. The x-position is not gauged against the beamline axis.

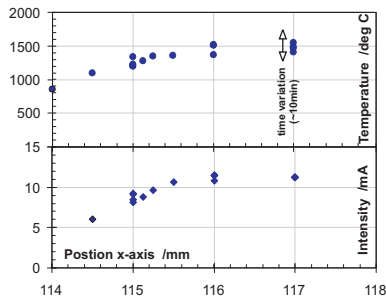


Figure 6: Due to high thermal load onto the needle it starts glowing. The temperature rise was measured with an optical pyrometer over the whole spectrum. Current was also measured, the shown variations arose in a time scale of minutes.

measurements [8] and caused by an in-homogeneously extracted ion beam amplified by the post acceleration which produces a focus in the horizontal plane close to the measurement point of the needle-BPM. Another prove is the integrated current of the BPM which is within $\approx 5\%$ of the toroid current (for profiles with step sizes where either the space was fully covered or oversampled and deconvoluted).

This focus is most likely the cause to let the needle glowing. Hence, an optical pyrometer was installed for temperature measurements to estimate thermal electron emissivity. The necessary data of W and its alloys to correct pyrometer reading and the calculations for the emissivity were taken from [9]. The results are shown in Fig. 6. Despite the peaky beam distribution the curve increases with a relatively moderate gradient. The thermal emission is described by the Richardson equation

$$J = A_G T^2 e^{-\frac{W}{kT}} \quad \text{with} \quad A_G = \lambda_B (1 - r_{av}) A_0. \quad (1)$$

In Fig. 7 the current density J is converted into a current to make it more comparable with Fig. 5. The used alloy has a small amount of Th which lowers the work function than that pure W. Assuming this worst case of 2 eV and a temperature of 2000°C the emission is far less than 1 mA. This would imply that the measurements are not significantly falsified.

SUMMARY AND OUTLOOK

The paper discussed an idea how to build a tomographic BPM consisting needle which can freely rotated and moved through the beam. First 1D beam profiles were taken. Thermal emission may contribute to the measurements but calculations imply a relatively small amount. This should be relatively easy to improve by choosing pure Tungsten.

It is envisaged that the DAQ and control for the Needle Scanner (and other FETS experiments) will be performed on a PXI-based DAQ system. PXI is chosen, rather than using PCI cards in a PC, since there are busses to synchronise triggers and clocks between multiple cards. The PXI controller can either be a 'slot-1' module, acting as a Windows-based PC and controlling the PXI system, or a desktop PC

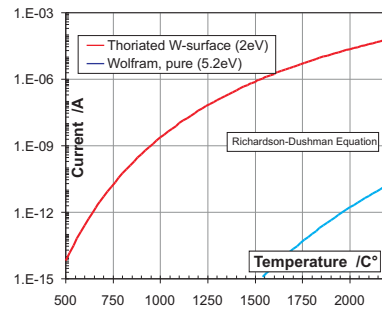


Figure 7: Emissivity of thermal electrons according to the Richardson-Dushman equation ($\varnothing \times l = 120 \text{ mm}$ was assumed for worst-case scenario; the beam is usually $\leq 50 \text{ mm}$

with a PCI-to-PXI extension. The ADC will be upgraded to a card capable of sampling at least 100 kSa/s , with a total noise of better than 0.5 mV (NI PXI-6251 or similar).

Future work will consist of changing the system to have each element (stage, temperature probe, pressure sensor, ADC channel etc) set up as an EPICS (or similar) server, and any Control/DAQ program to be a client of each server.

REFERENCES

- [1] A.P. Letchford et.al., "Status of the RAL Front End Test Stand", IPAC 2012, New Orleans, May 2012, THPPP051.
- [2] C. Gabor, D.A. Lee, J.K. Pozimsik, A.P. Letchford, "Laser-Based Beam Diagnostics for the Front End Test Stand (FETS) at (RAL)", EPAC 2006, Edinburgh, May 2006, TUPCH019.
- [3] D.A. Lee, J.K. Pozimski, C. Gabor, "A Laser Based Beam Profile Measuring Instrument for the Front End Test Stand at RAL", PAC09, Vancouver, BC, Canada, May 2009, TH5RFP051.
- [4] C. Gabor, A. Bosco, G. Boorman, G. Blair, A.P. Letchford, "A Non-Destructive Photo Detachment Laserwire for H-Ion Beams", BMW2010, Santa Fee, NM, USA, May 2010, TUPSM006.
- [5] C. Gabor, A. Bosco, G. Boorman, G. Blair, A.P. Letchford, "Status Report of the RAL Photo-Detachment Beam Profile Monitor", HB 2010, Morschach, Switzerland, Sept. 2010, WEO1C02, <http://hb2010.web.psi.ch/proceedings/index.htm>
- [6] A.C. Kak, M. Slaney, "Principles of Computerized Tomographic Imaging", IEEE Press, 1988.
- [7] C. Gabor, D. Reggiani, M. Seidel, A.P. Letchford, "Comparative Studies of Reconstruction Methods to Achieve Multi-Dimensional Phase Space Information", DIPAC11, Hamburg, Germany, May 2011, TUPD91
- [8] C. Gabor, D.C. Faircloth, S.R. Lawrie, A.P. Letchford, "Diagnostics experiments at a 3 MeV test stand at Rutherford Appleton Laboratory, UK", ICIS 2009, Rev. Sci. Instr. Vol. 81, 02B718, Feb. 2010
- [9] E. Lassner, W.D. Schubert, "Tungsten: Properties, Chemistry and Technology of the Element", 1999 Kluwer Academic/Plenum Publisher, New York